

The "laser greenhouse" thermonuclear target with distributed absorption of laser energy

S. Yu. Gus'kov, N. V. Zmitrenko, and V. B. Rozanov

P. N. Lebedev Institute of Physics, Russian Academy of Sciences, 117924 Moscow, Russia
(Submitted 12 April 1995)

Zh. Éksp. Teor. Fiz. **108**, 548–566 (August 1995)

We propose a new type of target for laser-driven thermonuclear fusion, which can ensure uniformity in the distribution of laser energy absorbed by the target and thus uniformity in the pressure required to compress the thermonuclear material (fuel). A distinctive component of this target is a special absorber of laser radiation placed between an external inertial shell and an internal spherical capsule that contains the thermonuclear material. Laser radiation is introduced into the absorber through apertures in the external shell. The absorber consists of low-density material (e.g., a porous material or gas) made up of light elements with a density lower than the critical density of the plasma formed by the laser. The distribution of absorbed energy is equalized by propagation of supersonic electron thermal conduction waves as distributed inverse-bremsstrahlung absorption of the laser radiation takes place in the subcritical plasma of the absorber. Our theoretical studies have shown that for a target with a high thermonuclear gain coefficient $G \geq 1$, thermal equilization of nonuniformities in the plasma heating is possible even when a laser with as few as six beams is used. The target we propose has excellent energy characteristics: one-dimensional numerical calculations show that the threshold value of laser energy for the ignition of this type of target is 100–200 kJ, i.e., considerably smaller than that required for indirect drive. Moreover, calculations show that the gain coefficient increases rapidly for this type of target with increasing laser energy. Thus, for a laser energy of 1 MJ the amplification coefficient is approximately equal to 50. © 1995 American Institute of Physics.

1. INTRODUCTION

In order to stably compress a spherical thermonuclear target using beams of laser radiation or ion beams, it is necessary to ensure that the energy deposition by these drivers in the target is highly uniform. Specifically, the nonuniformity of the target heating should not exceed 1–3 percent.¹

Studies of laser thermonuclear fusion that attempt to address this problem are based, at the present time, on two approaches. In the first approach, effort is focused on ensuring a high degree of uniformity in the laser illumination of the target. Contemporary experiments have made use of so-called "optical equalization" methods, in which the laser beam is made to pass through special optical elements (various types of phase plates, spectrally dispersive elements, etc.). These elements cause the output laser beam to have a high degree of uniformity in the energy distribution over its cross section, to the point where nonuniformity of this distribution is no more than a few percent.^{2–4}

However, numerical calculations and experiments show that when the laser radiation acts directly on the target the required degree of uniformity of the energy deposited in the target can be achieved only by illuminating the latter with a large number of laser beams, up to several dozen.⁵ This greatly complicates the systems that control radiation from the laser driver, and consequently increases its cost considerably.

Another approach is to first convert the radiation from the laser into soft x -rays, which transfer energy to the target with a high degree of isotropy, thereby compressing the latter

isotropically (i.e., so-called indirect drive).⁶ It should be noted that all contemporary efforts to achieve heavy-ion thermonuclear fusion are based on indirect-drive schemes in which ion beam energy is converted into x -ray energy. The transformation of the energy of a laser or ion driver to x -ray energy is accomplished in a special converter, which can either be separate from the thermonuclear target⁶ or a part of the latter.^{7,8}

However, in indirect drive the high degree of uniformity of target heating must be paid for by the loss of 70–80% of the useful energy in the process of converting the laser radiation to x -rays. Thus, whereas the threshold for ignition of a thermonuclear target (i.e., liberation of thermonuclear energy equal to the injected laser energy) theoretically corresponds to a laser energy of 100–200 kJ for spherically symmetric direct drive,⁹ for indirect drive this number is 0.6–1.5 MJ.^{4,5,10}

In this paper we propose a new approach to the problem of uniformly depositing laser energy in a target, in which the nonuniformities arising from direct illumination of the target by laser beams are smoothed out through transport of energy by supersonic electronic thermal conduction waves. This process takes place when the laser radiation is absorbed in a subcritical extended plasma generated by a special absorber.^{11,12} We claim that an additional hydrodynamic process takes place in this target, arising from the nonuniform distribution of mass and (or) density in the shell that compresses the thermonuclear material (fuel), that compensates for nonuniformities in the compression.^{11,12}

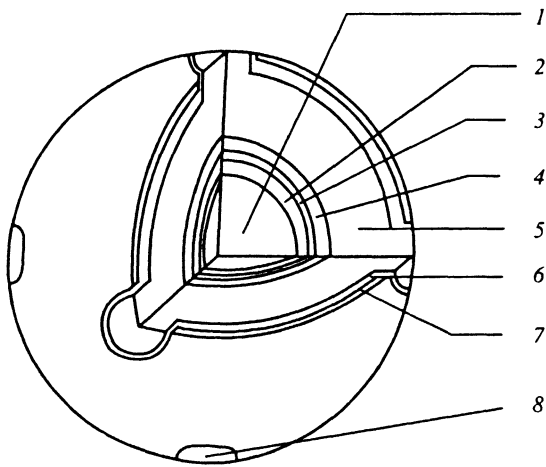


FIG. 1. Sketch of laser greenhouse target. Thermonuclear capsule: 1—DT gas, 2—DT ice, 3—layer of high- z material (e.g., copper) or a layer of light-element material (for example, polyethylene) containing impurities of heavy elements; 4—ablator made of light-element material (for example, a polyethylene layer). The absorber 5 consists of a low-density light-element material (porous material or gas). External inertial shell: 6—inner layer made of light-element material (for example, a polyethylene layer); 7—external layer made of material with high density (for example, a copper layer); 8—aperture for input of laser beams.

2. OVERALL PICTURE OF PHYSICAL PROCESSES

In traditional laser-driven direct-drive schemes,⁹ the thermonuclear target consists of a spherical capsule containing the thermonuclear material, either DT gas occupying a cavity in the capsule or DT ice frozen onto the inner surface of the capsule. The capsule itself is a spherical shell consisting of several concentric layers of different materials. The outer layer of the shell, the ablator, is designed to generate pressure as its material is heated and vaporized by the laser pulse. There may be several layers within the shell as well, among them a layer consisting of heavy elements (or containing impurities of heavy atoms) designed to absorb the intrinsic radiation of the plasma from the heated regions of the target.

Absorption of the laser radiation takes place in the ablator material, which expands towards the laser beam (opposite the direction of propagation) near the region with critical density. Under the action of ablation pressure, the target material is compressed towards the center. By making the ablator material out of light elements, we ensure on the one hand that acceleration of the target material takes place with high hydrodynamic efficiency, while on the other hand minimizing the amount of thermal energy radiated by the ablator plasma.

Our target concept, a sketch of which is shown in Fig. 1, differs from previous designs in two fundamental respects. The first is that we add an additional element to the traditional direct-drive target scheme—a special absorber of laser radiation with the ability to equalize the distribution of energy absorbed by it from a preset number of laser beams in a given illumination geometry. The absorber, which surrounds the capsule of thermonuclear material, consists of a spherical layer of light-element material with an initial density lower

than the critical density of the plasma that forms during absorption of laser radiation with a given wavelength.

In order to increase the energy efficiency of the target by retarding the departure of absorber material from the outer portion of the absorber, a massive shell is deposited on top of the latter with apertures for the input of laser radiation to the target. This outer shell, like the shell of the internal thermonuclear capsule, should consist of at least two layers: an outer layer of heavy-element material, which provides inertia for the shell, and an inner layer consisting of light-element material (e.g., polyethylene in the normal state) that prevents the thermal wave from penetrating the absorber into the outer shell, thereby decreasing the thermal energy radiated by the target.

As an absorber either a porous material (e.g., porous polyethylene) or a gas can be used. In the latter case, the input aperture should be closed by a thin layer of light material which should burn through and evaporate within a time considerably less than the duration of the laser pulse.

A second feature of our target scheme is the use of a nonuniform shell for the thermonuclear capsule (ablator) for additional smoothing of nonuniformities in the target heating that remain after the equalizing action of the absorber. The mass or density distributions of ablator material should be chosen from the condition that they compensate pressure nonuniformities as the ablator is accelerated, i.e., the distribution of these quantities should be close to that of the ablation pressure.

Variations in the distribution of laser energy in the absorber are smeared out because supersonic electron thermal conduction waves can propagate in the low-density material, with temperatures at the wave front that exceed 1 keV. As we will show below, for targets that correspond to a gain exceeding unity, these waves, which remain supersonic, can bring about transverse (with respect to the target radius) equalization of the temperature between adjacent regions where laser radiation is absorbed before the waves can leave the ablator surface, even when the number of laser beams k is relatively small, i.e., $k \geq 6$.

For laser intensities and wavelengths corresponding to the condition $I\lambda^2 \leq 10^{14} \text{W} \cdot \mu\text{m}^2/\text{cm}^2$ (which implies that parametric interactions between the laser radiation and the plasma¹³—e.g., induced scattering of the laser radiation and generation of “hard” electrons play little role—and make small negative contributions to the compression of the thermonuclear target associated with them), the plasma can be heated to temperatures exceeding 1 keV only in a regime of laser radiation absorption where practically all the absorbed energy resides in the thermal component (i.e., the “heating” absorption regime).¹⁴ This is easy to see by comparing the laser energy flux with the electronic thermal conduction flux.

The process by which a solid material (with supercritical density) absorbs radiation under the action of a laser pulse involves a different so-called “hydrodynamic” absorption regime. This regime is accompanied by hydrodynamic expansion of material in the form of a plasma flux with subcritical density, during which a significant fraction of the absorbed energy (up to 70%) is converted to kinetic energy of hydrodynamic motion.¹⁴

In this paper, we propose to use an absorber with subcritical density to achieve this "thermal" regime of absorption of the laser radiation. In this case, the radiation is absorbed almost simultaneously over the entire inverse-bremsstrahlung absorption length ("bulk" absorption), without the preliminary conversion of material into subcritical plasma that occurs when laser radiation is absorbed by a solid body.

Thus, during absorption by the subcritical absorber, laser radiation penetrates into the target through openings in the outer shell to a distance equal to the inverse-bremsstrahlung absorption length (which for harmonics of the Nd laser is several tens of microns) along the direction of incidence of the laser beams on the target. The absorbed energy is distributed simultaneously over the entire bulk of the absorber by high-power electron thermal conduction waves. Starting from this picture of physical processes in the absorber, we have called this type of target a laser greenhouse target, or LIGHT (Laser Irradiated Greenhouse Target).

Let us note here that during direct compression of a traditional target, indirect compression of a target, and compression of a "laser greenhouse" target, the physical principles that operate involve conversion of the laser energy into different forms of target energy. In the first case, the laser energy is converted directly into kinetic energy of the plasma generated by the evaporating portion of the target, which gives rise to the reactive pressure pulse required for compression. In indirect compression, the laser energy is first converted to x -ray energy, while in the laser greenhouse target it is converted into plasma thermal energy.

Conversion of laser energy into plasma thermal energy was the basis for the earliest proposal involving inertial thermonuclear fusion, put forth by Basov and Krokhin¹⁵ in the mid-1960's. However, direct heating of DT plasmas without compression of the thermonuclear material can lead to gains of ~ 1 only at laser energies of 100–200 MJ.

In a laser greenhouse target, laser energy is converted to thermal plasma energy in order to ensure stable compression of the thermonuclear material under conditions of higher energy concentration and higher ablation pressures than for indirect laser targets.

In this paper we give a theoretical description of the operating principles of a laser greenhouse target. Using analytic models, we discuss the fundamental physical processes that occur in a target of this type:

- 1) generation of a uniform plasma in the course of bulk inverse-bremsstrahlung absorption of laser radiation by a porous material with subcritical macrodensity;
- 2) initiation and propagation of supersonic electron thermal conduction waves from the regions of where the laser beams are absorbed;
- 3) equalization of the temperature distribution in the absorber in the direction transverse to the propagation of the laser beam;
- 4) generation of ablation pressure in a laser greenhouse target; and,
- 5) intrinsic thermal radiation.

The energetic efficiency of the target is discussed in terms of the numerical calculations.

3. GENERATION OF A PLASMA BY LASER RADIATION ACTING ON A MATERIAL WITH SUBCRITICAL MACRODENSITY

Let us consider the process of evaporation of a porous absorber under the action of laser radiation. As a model we will assume that the porous material is made up of a collection of particles of absorber material in their normal state with characteristic sizes smaller than the distance between particles:

$$\frac{b_0}{d_0} \approx \left(\frac{\rho_*}{\rho_0} \right)^{1/3}$$

Here b_0 and d_0 are, respectively, the average size of the absorber material particles and the distance between them, ρ_* and ρ_0 are, respectively, the macrodensity (i.e., mean density) of the absorber in the porous state and the density of the absorber in the normal state (for example, $\rho_0 \approx 1 \text{ g/cm}^3$ for polyethylene).

When laser radiation strikes a planar layer of porous material, N_0 particles evaporate simultaneously from a total cross sectional area that covers the area of the beam cross section:

$$N_0 = S_L / b_0^2,$$

where S_L is the cross sectional area of the laser beam; these particles may be located at various distances from the external surface layer. Within the evaporation time, these particles absorb an energy

$$E_{e0} \approx S_L I t_{e0},$$

where I is the intensity of the absorbed laser radiation, and t_{e0} is time it takes for N_0 particles to evaporate. In this case the energy of hydrodynamic motion of the evaporated particles equals

$$\rho_0 v^2 b_0 S_L \approx [2(\gamma - 1)/(3\gamma - 1)] E_{e0}, \quad (1)$$

where v is the velocity of hydrodynamic motion of the evaporated material^{14,16} and γ is the adiabatic index.

The process of evaporation from a porous layer differs considerably from solid-layer evaporation. Evaporation from a solid layer is accompanied by planar expansion of material, while evaporation of material in the porous state involves bulk expansion of individual absorber macroparticles. The collision of neighboring macroparticle fluxes leads to rapid thermalization of the macroparticles. As a result, the time for evaporation and expansion of macroparticles from a porous material to form a plasma with density ρ_* is

$$t_{e0} \approx \frac{b_0}{v} \left(\frac{\rho_0}{\rho_*} \right)^{1/3}. \quad (2)$$

Using (1) and (2), we obtain a relation between the flow velocities when porous and solid layers evaporate to form plasmas with the same final density ρ_* :

$$v \approx v_c (\rho_* / \rho_0)^{1/6}. \quad (3)$$

Here $v_c = [2(\gamma - 1)I / (3\gamma - 1)\rho_*]^{1/3}$ is the velocity of the material particles as they evaporate from the solid layer.^{14,16}

To sum up, the total time it takes to generate a plasma with density ρ_* by evaporation of a porous layer of material with thickness h is

$$t_e = \frac{S_L h}{d_0^3 N_0} t_{e0} \approx \sqrt{\frac{\rho_*}{\rho_0}} h \left[\frac{2(\gamma-1)I}{(3\gamma-1)\rho_*} \right]^{-1/3}. \quad (4)$$

The time for evaporation and expansion of a solid layer with density ρ_* is

$$t_{ec} = \frac{h}{v_c} \approx h \left[\frac{2(\gamma-1)I}{(3\gamma-1)\rho_*} \right]^{-1/3}. \quad (5)$$

For the ratio of evaporation times we obtain

$$\frac{t_e}{t_{ec}} = \sqrt{\frac{\rho_*}{\rho_0}} \ll 1. \quad (6)$$

Thus, bulk evaporation of a porous layer creates a plasma much more rapidly than planar evaporation of a solid material with the same mass and atomic composition. For example, according to (6), when porous polyethylene with a macrodensity $\rho_* = 3 \cdot 10^{-2} \text{ g/cm}^3$ evaporates, plasma creation takes place roughly six times as fast as when the same mass of polyethylene in the form of a layer with normal density $\rho \approx 1 \text{ g/cm}^3$ evaporates to form a plasma with density ρ_* .

There is one more important circumstance worth noting when a plasma is created by absorption of laser radiation in the internal low-density absorber of a laser greenhouse target. During bulk evaporation of a porous absorber, the uniform plasma is generated in a time much shorter than the time for leakage of material through the apertures that admit the laser beams into the target. Actually, this leakage time t_d is determined by the transit of ions of the material across the entire thickness of the layer h :

$$t_d = \frac{h}{v} \approx h \left(\frac{\rho_0}{\rho_*} \right)^{1/6} \left[\frac{2(\gamma-1)I}{(3\gamma-1)\rho_*} \right]^{-1/3}. \quad (7)$$

The time (4) to generate the plasma is determined by the time it takes the ions to cross the distance between neighboring absorber macroparticles, i.e., a distance considerably smaller than the layer thickness h . Therefore, by setting the leakage time (7) equal to the time (4) for creating the plasma, we readily obtain

$$\frac{t_e}{t_d} = \left(\frac{\rho_*}{\rho_0} \right)^{2/3} \ll 1.$$

Numerical estimates show that when a laser pulse at the third harmonic of a Nd laser with intensity $I = 5 \cdot 10^{14} \text{ W/cm}^2$ is incident on a porous ablator with density corresponding to the critical density $\rho_* = 3 \cdot 10^{-2} \text{ g/cm}^3$, a uniform plasma is generated in a time $\sim 10^{-10} \text{ s}$, i.e., much shorter than the required duration of the laser pulse, which is several nanoseconds.

The coefficient of inverse bremsstrahlung absorption of laser radiation in a plasma with subcritical density is¹⁷

$$K_a \approx \frac{\nu_{ei}}{c} \left(\frac{\omega_p}{\omega_L} \right)^2, \quad (8)$$

where

$$\nu_{ei} \approx 6 \cdot 10^{14} \frac{\rho z^2}{A T^{3/2}} \text{ s}^{-1} \quad (9)$$

is the frequency of electron-ion collisions (in s^{-1}), and z and A are, respectively, the degree of ionization and atomic number of the plasma ions. Here and in what follows, the plasma temperature T is given in keV; c is the velocity of light (cm/s); ω_p and ω_L are the plasma frequency and laser radiation frequency, respectively; and we have used $(\omega_p/\omega_L)^2 \approx 5.4 \cdot 10^2 z \rho \lambda^2/A$, where λ is the wavelength of the laser radiation (μm).

The size (in cm) of the region of absorption of the laser radiation $h_a = K_a^{-1}$, according to (8), is

$$h_a \approx 9.2 \cdot 10^{-8} A^2 T^{3/2} / z^3 \lambda^2 \rho^2. \quad (10)$$

For a plasma with critical density $\rho_* = \rho_c = 1.6 \cdot 10^{-3} A / z \lambda^2$, it follows from (10) that

$$h_{ac} [\text{cm}] \approx 3.1 \cdot 10^{-2} T^{3/2} \lambda^2 / z. \quad (11)$$

Calculations using Eq. (11) for the size of the region in which laser radiation from a Nd laser with $\lambda = 0.35$ to $1.06 \mu\text{m}$ is absorbed in a plasma with critical density and a temperature ~ 1 to 2 keV gives a range of values 30 to $100 \mu\text{m}$, respectively. This range corresponds to a lower limit of the thickness of the absorber for a laser greenhouse target.

4. EQUALIZATION OF NONUNIFORMITIES IN THE LASER HEATING OF A MATERIAL BY THERMAL CONDUCTION IN THE LASER GREENHOUSE TARGET

Let us consider the process by which the temperature distribution of the plasma in the absorber of a laser greenhouse target is equalized through the propagation of electronic thermal-conduction waves away from the region of absorption of the radiation. We will assume that the target has k openings to admit the laser beams. The process of propagation of electron thermal-conduction waves, which is initiated as the plasma is heated by an individual laser beam, can be treated approximately as the generation of a spherical thermal wave from a point source if the size R_κ of the region occupied by the thermal wave is larger than the size h_a of the region in which the laser light is absorbed. For $h_a \ll R_\kappa$ this problem resembles the self-similar problem of an instantaneous point source of heat,¹⁸ with the difference that the action of the laser radiation causes the energy of the region occupied by the thermal wave to increase with time, so that the solution given in Ref. 18 cannot precisely describe the process under discussion (taking into account all the profile coefficients). Nevertheless, it is easy to obtain a rather accurate estimate by averaging the thermal-conduction equation over the region occupied by the thermal wave. In this case it is sufficient to assume that energy is liberated within a region ($h_a < R_\kappa$), and not necessarily at a point ($h_a \ll R_\kappa$).

The energy of the spherical region under discussion is

$$E_L = \frac{4\pi}{3} R_\kappa^3 \rho B_a T_\kappa,$$

where T_κ is the average temperature of the electrons in the region of the thermal wave. The equation for R_κ follows from the general considerations of Ref. 18:

$$\frac{dR_\kappa^2}{dt} = \frac{4}{n} \frac{\kappa_e}{\rho B_a},$$

which is exact for the problem of an instantaneous heat source. Here $\rho = \rho_*$ is the density in the region of the thermal wave, $\kappa_e = \kappa T^n$, where $n=2.5$, and $\kappa \approx 10^{19}/(z+4)$ is the coefficient of electron thermal conductivity in units of erg/keV^{7/2}cm·s; $B_a = 10^{15}(z+1)/A(\gamma-1)$ is the specific heat in units of erg/g·keV.

From this it is easy to obtain the following expression for R_κ :

$$R_\kappa = \left[\frac{6n+4}{n} \kappa_a \left(\frac{3}{4\pi} \right)^n \frac{1}{(\rho B_a)^{n+1}} \int_0^t E^n dt \right]^{1/(3n+2)},$$

where

$$E(t) = S_L \int_0^t I(t) dt.$$

For the case of a constant flux I we have for $n=2.5$

$$R_\kappa = \left[\frac{76}{35} \left(\frac{3}{4\pi} \right)^{5/2} \frac{\kappa_a (IS_L)^{5/2}}{(B_a \rho_*)^{7/2}} \right]^{2/19} t^{7/19}, \quad (12)$$

$$T_\kappa = \left[\frac{35}{76} \left(\frac{3}{4\pi} \right)^{2/3} \frac{(IS_L)^{2/3} (B_a \rho_*)^{1/3}}{\kappa_a} \right]^{6/9} t^{-2/19}. \quad (13)$$

We note that, for $I(t) = I_0 t$ (this dependence is used in the numerical simulation, see Sec. 8), we have $R_\kappa \propto t^{12/19}$, $T_\kappa \propto t^{2/19}$.

In order to study the dynamics of heating of the absorber material in a laser greenhouse target, we will compare the radius of the thermal wave front with the size of the region where the laser radiation is absorbed. Substituting into (10) the expression for the temperature at the thermal wavefront (13), we obtain for the size of the absorption region

$$h_a \approx 1.7 \cdot 10^{-12} \left(\frac{A}{z} \right)^{35/19} \frac{(z+4)^{9/19} (IS_L)^{6/19}}{z \lambda^2 \rho_*^{35/19} (\gamma-1)^{3/19}} t^{-3/19}. \quad (14)$$

In this case the ratio h_a/R_κ , taking (12) into account, is:

$$\frac{h_a}{R_\kappa} \approx 9 \cdot 10^{-11} \left(\frac{A}{z} \right)^{28/19} \times \frac{(z+4)^{11/19} (IS_L)^{1/19}}{z \lambda^2 \rho_*^{28/19} (\gamma-1)^{10/19}} t^{-10/19}. \quad (15)$$

This result shows that there is a short time period at the beginning of the process when the size of the heated plasma in the radial direction (in the direction of propagation of the laser beam) is determined by the absorption length of the laser radiation. At the end of this time, an electron thermal-conduction wave moves in the radial direction, which propagates ahead of the absorption wave front. For $I \approx 5 \cdot 10^{14}$ W/cm², $\lambda = 0.35 \mu\text{m}$ and a beam cross sectional radius $R_L \approx 300$ to $500 \mu\text{m}$, the time it takes to generate the thermal wave is about $(2-5) \cdot 10^{-11}$ s, i.e., considerably shorter than the laser pulse.

A criterion for equalization of nonuniformities in the heating of the absorber material obviously follows if we assume that the thermal-conduction wave propagates from the

region where the laser radiation is absorbed over a distance equal to half the distance between neighboring regions of the absorber within a time shorter than the duration of the laser pulse. The distance between regions where the laser radiation is absorbed approximately

$$\Delta \approx \sqrt{\frac{4}{k}} (1 - \sqrt{\sigma}) R, \quad (16)$$

where $\sigma = kR_L^2/4R^2$ is the relative area of the input apertures to the target, k is the number of input apertures, and R is the target radius.

According to (12) and (16), the time (in seconds) for thermal wave fronts propagating from neighboring regions of absorption of the laser radiation to converge is

$$t_\kappa \approx 7.4 \cdot 10^3 \left(\frac{z\rho_*}{(\gamma-1)A} \right) \frac{(1-\sqrt{\sigma})^{19/7} (z+4)^{2/7} R^{9/7}}{k^{9/14} I^{5/7} \sigma^{5/7}}, \quad (17)$$

and the criterion for equalization can be written

$$R < 3 \cdot 10^{-2} \left[\frac{(\gamma-1)A}{z\rho_*} \right]^{7/23} \times \frac{E_L^{7/23} k^{9/46}}{(z+4)^{2/23} (1-\sqrt{\sigma})^{19/23} (I\sigma)^{2/23}}. \quad (18)$$

Here E_L is the energy (in J) of the laser radiation from all the beams, I is in W/cm², and R in cm.

The criterion for equalization of the absorber temperature (18) gives a value for the upper limit of the radius of a "laser greenhouse" target. Thus, when the number of Nd laser beams used is six, each with a wavelength $\lambda = 0.35 \mu\text{m}$, $I = 10^{15}$ W/cm², and $E_L = 10^5$ J, and the absorber has a density $\rho = 3 \times 10^{-2}$ g/cm³ and charge state $z=3$, the target radius must be no larger than 0.18 cm. The maximum radius of the outer shell of a Laser Greenhouse target is considerably greater than that of the thermonuclear capsule containing the DT fuel, which lies in the range 0.07–0.1 cm for an energy of 10^5 J. This suggests that there is a fairly broad range of possibilities for optimizing the parameters of a Laser Greenhouse target. For the laser beam and absorber parameters given above and a target radius of 0.1 cm, the time required for the thermal wavefronts to converge is 0.1 ns, i.e., substantially less than the laser pulse length. The target has a relative aperture area $\sigma = 10\%$.

There are two types of laser greenhouse target that differ in regard to the absorber thickness. In the first type, the absorber thickness must exceed the distance between the shells for absorption of laser energy; in the second type, the absorber thickness must be smaller than this distance. The first target type ensures complete symmetrization of the ablator heating, since in this case the thermal wave exits the ablator surface after equalizing the temperature distribution in the transverse direction behind its front. In this type of target, the relative thickness of the absorber (with respect to target radius) decreases as the number of input apertures and their relative cross-sectional areas increase [see (16)]: for $k=6$ and $\sigma=0.1$, we have $h \approx 0.55 R$, while for $k=12$ and $\sigma=0.2$, we have $h \approx 0.3 R$. The second target type corresponds to incomplete symmetrization of the ablator heating,

since the thermal waves exit the surface of the ablator before their fronts converge in the transverse direction. In this case, we can compensate the nonuniformity of the ablator heating by a special distribution of ablator mass, i.e., by proper choice of the shape and density distribution of the material. Note that although the procedure by which it achieves uniform ablator heating is more complicated, the second target type may be capable of producing a higher concentration of energy in the absorber than the first type.

5. INTRINSIC RADIATION

In optimizing the parameters of a laser greenhouse target, it is important to minimize the level of intrinsic plasma radiation. For a target of this type, conversion of laser energy to thermal radiation from the plasma is energy loss mechanism. Furthermore, the intrinsic radiation is an additional source of entropy (in connection with the shock wave), which is transferred to the compressed material of the thermonuclear target.

The primary sources of thermal radiation in the laser greenhouse target are regions of dense heated plasma that form when the inner layer of the external shell and the external ablator layer of the thermonuclear capsule are burned through by the electron thermal-conduction waves from the absorber. The thermal energy irradiated by the absorber itself is insignificant due to its low density. Simple estimates show that this energy is less than 1 to 2% of the absorbed energy. However, it is important to note that the spectrum of thermal radiation by the absorber, which corresponds to a plasma temperature of 1 to 3 keV, is quite broad.

The characteristics of the thermal radiation from both shells of the target are similar. Let us estimate them for the case of the external shell. The radiating layer of plasma created at the outer shell arises from two processes: propagation of the electron thermal-conduction wave from the absorber into the shell, and hydrodynamic expansion of heated material from the shell toward the low-density absorber. Using the self-similar solution (12), (13) as the initial approximation, it is easy to determine the ratio of energy transported by the thermal wave into the shell to the total energy absorbed in the absorber (χ), and also the thickness of the layer of shell burned through by the thermal wave (δ):

$$\chi \approx 1 - \beta^{2/9}, \quad (19)$$

$$\delta \approx 0.25 \beta^{7/9} (1 - \beta^{2/9}) R_\kappa \frac{\kappa_s}{\kappa_a}. \quad (20)$$

In these expressions

$$\beta = 4 \frac{\kappa_a \rho B_a}{\kappa_s \rho_{s0} B_s}$$

κ_s , B_s , and ρ_{s0} are the thermal-conductivity coefficient, the specific heat, and the initial density of the material of the outer shell, respectively, while R_κ is determined from Eq. (12).

If the expansion of the heated layer of the shell within the target is treated in the adiabatic approximation, it is easy to obtain the following expressions for the plasma parameters of this layer

$$T_s \approx \left(\frac{\rho B_a}{\rho_{s0} B_s} \right)^{(\gamma-1)/\gamma} \beta^{2/9} T_\kappa, \quad \rho_s \approx \left(\frac{\rho B_a}{\rho_{s0} B_s} \right)^{1/\gamma} \rho_{s0}, \quad (21)$$

where T_κ is determined from Eq. (13).

Calculations based on Eqs. (20), (21) for a shell inner layer made of plastic ($\rho \approx 1 \text{ g/cm}^3$), a target radius $R = 0.15 \text{ cm}$, an absorber density $\rho_{s0} \approx 10^{-2} \text{ g/cm}^3$, a laser intensity $I \approx 10^{15} \text{ W/cm}^2$, a wavelength $\lambda = 0.35 \text{ } \mu\text{m}$, and a pulse duration $\tau_L = 3 \text{ ns}$ give a value of 8 to 12 μm for the thickness of the outer shell layer burned through by the thermal-conduction wave, and the values (0.05-0.1) g/cm^3 and (800-400) eV for the density and temperature of the resulting plasma, respectively. The bremsstrahlung energy of a plasma with these parameters within the time of the laser pulse is $\sim 3-5\%$ of the energy absorbed in the target.

Thus, the intrinsic radiation energy of a laser greenhouse target exceeds that of a traditional direct-drive target¹⁹ by a factor of roughly 1.5, and this makes up a small portion of the total energy absorbed by the target. The intrinsic radiation energy from the burned-through layers of the shell is effectively absorbed in the compressed portion of the ablator of the thermonuclear capsule within a relatively narrow spectral range corresponding to a plasma temperature $\sim 800-400 \text{ eV}$; moreover, like the intrinsic radiation in a traditional direct-drive target, its role in the transport of absorbed energy is insignificant, and it has practically no negative effect on the compression of the thermonuclear plasma. Nevertheless, additional shielding of the compressed plasma from burn-through by the absorber radiation is required, because the latter possesses a wide spectrum. This is achieved by building an inner layer into the ablator structure of the thermonuclear target; this layer, which contains heavy elements, makes up 20 to 30% of the mass of the entire ablator for a working target (by mass).

6. HYDRODYNAMIC PROCESSES IN THE ABSORBER OF A LASER GREENHOUSE TARGET

We now discuss our criteria for choosing the parameters of the laser greenhouse target absorber. Our choice should be one that minimizes the effect of hydrodynamic perturbations on the processes by which thermal conduction equalizes the temperature distribution in the absorber; more generally, we will require that the "thermal" regime of absorption of the laser radiation to minimize the conversion of absorbed energy into energy of hydrodynamic motion of material within the time the laser pulse acts.

The first requirement implies that the velocity of the thermal wave must exceed the shock-wave velocity while the temperature in the absorber is being equalized, i.e., before the fronts of the transverse thermal waves have converged. The regime of supersonic thermal waves corresponds to the initial stage of this process, whose duration is the same order as the time for electron-ion energy exchange. Actually, the velocities of the thermal and shock waves can be estimated from the following well-known expressions, respectively:

$$v_\kappa \approx \sqrt{\frac{v_e^2 \tau_{ei}}{t}}, \quad D = v_s \sqrt{\frac{\gamma+1}{2}}.$$

Here $\tau_{ei} = \nu_{ei}^{-1}$ is the electron-ion collision time [see (9)], $v_e = \sqrt{3T_e/m_e}$ is the thermal velocity of electrons, and $v_s = \sqrt{zT_e/m_i}$ is the isothermal velocity of sound.

Thus, the condition for existence of an ultrasonic electron thermal-conduction wave $v_\kappa > D$ is fulfilled for times

$$t \leq t_s, \quad t_s = [4/z(\gamma+1)]\tau_E,$$

where $\tau_E = (m_i/2m_e)\tau_{ei}$ is the time for energy exchange between the electronic and ionic components of the plasma.²⁰ The structure of subsonic and supersonic thermal-conduction waves was discussed in Ref. 21 using the self-similar solution to the hydrodynamic equations obtained there.

Using Eq. (9) for τ_E , we can write t_s in the form

$$t_s[\text{s}] \approx 1.2 \cdot 10^{-11} \left(\frac{A}{z}\right)^2 \frac{T^{3/2}}{z\rho_*(\gamma+1)}.$$

It is easy to see that for $\rho_* \approx 3 \cdot 10^{-3} - 3 \cdot 10^{-2} \text{ g/cm}^3$ and $T = 1 - 2 \text{ eV}$ the stage of ultrasonic thermal waves lasts 0.5 to 8 ns, i.e., longer than the time for temperature equalization $t_\kappa \approx 0.3 \text{ ns}$ (see Sec. 4) and comparable to the duration of the laser pulse.

Let us do a more detailed calculation. Calculations based on Eqs. (12) and (13) give the following expressions for the velocities of the thermal and sound waves (in cm/s)

$$v_\kappa \approx 7 \cdot 10^{-3} \left(\frac{(\gamma-1)A}{z\rho_*}\right)^{7/19} \frac{(IS_L)^{5/19}}{(z+4)^{2/19}} t^{-12/19},$$

$$v_s \approx 8.5 \cdot 10^5 \times \left(\frac{z}{(\gamma-1)A}\right)^{21/38} [\rho_* I^2 S_L^2 (z+4)^3]^{1/19} t^{-1/19},$$

the ratio of these quantities when the thermal wave fronts converge (see (17)) is

$$\frac{v_s}{v_\kappa} \approx 1.4 \cdot 10^{10} \left(\frac{z}{A}\right)^{3/2} \frac{\rho_*(1-\sqrt{\sigma})^{11/7} (z+4)^{3/7} R^{3/7}}{(\gamma-1)k^{3/14} I^{4/7} \sigma^{4/7}}. \quad (22)$$

When six beams of Nd-laser light with parameters $\lambda = 0.35 \mu\text{m}$, $I = 10^{15} \text{ W/cm}^2$, $E_L = 10^5 \text{ J}$ are incident on a target with a relative aperture area $\sigma = 10\%$ and an absorber with density $\rho_* \approx 3 \cdot 10^{-2} \text{ g/cm}^3$ and $z = 3$, even for the largest target radius we have $v_s/v_\kappa \approx 0.4$, i.e., hydrodynamic perturbations cannot outrun the thermal wave fronts before the latter converge, and cannot transport distortions in the symmetry of the transverse plasma pressure distribution away from the absorber. In this case, the fraction of thermal energy compared to the total energy at the thermal wave front, which we estimate to be

$$1 - kv_s^3 \Delta^2 / v_\kappa^3 R^2,$$

is 75 to 80%, i.e., the absorption and transport of laser energy takes place in the thermal regime. This also leads to high temperatures in the absorber plasma—in excess of 1 keV—which in turn smooths out the nonuniformities that appear when the material is heated by the laser beams at the required rate.

7. CONCENTRATION OF ENERGY AND ABLATION PRESSURE

If we neglect the dimensions of those portions of the external and internal shells that are burned through by the thermal wave ($\delta \ll h$, see Sec. 5), the time-averaged ablation pressure in a laser greenhouse target is determined by the degree of spatial concentration of the energy corresponding to the absorber thickness h :

$$P_{LGH} = (\gamma-1)E_L(t)/4\pi R^2 h. \quad (23)$$

Let us compare the values of the ablation pressure for a laser greenhouse target and a simple shell target directly illuminated by the laser. The ablation pressure for direct illumination of a spherical target is^{14,16}

$$P_d \approx 2[2(\gamma-1)/(3\gamma-1)]^{2/3} \rho_{cr}^{1/3} I^{2/3}. \quad (24)$$

Comparing (23) and (24), we obtain

$$P_{LGH} \approx 0.5 \left(\frac{3\gamma-1}{2}\right)^{2/3} \left(\frac{\rho_*}{\rho_{cr}}\right)^{1/3} \left(\frac{v_s t_L}{h}\right)^{2/3} P_d, \quad (25)$$

where

$$v_s = \sqrt{\frac{E(\gamma-1)}{4\pi R^2 h \rho_*}}.$$

In this case, when $\rho_* \approx \rho_{cr}$ we obtain the following pressure ratio:

$$\frac{P_{LGH}}{P_d} \approx \left(\frac{v_s t_L}{h}\right)^{2/3}. \quad (26)$$

For a laser greenhouse target with uniform burn-through of the absorber, when the fronts of the transverse thermal waves converge before exiting the surface of the ablator, the minimum value for the absorber thickness is $v_\kappa t_L \approx \Delta$. Therefore, according to (25) and (26) the ablation pressure for such a target is less than

$$P_{LGH} \approx P_d (v_s/v_\kappa)^{2/3}.$$

According to the results of the previous section, $v_s/v_\kappa \approx 0.4$; consequently, $P_{LGH}/P_d \approx 0.5$. Thus, it is typical for the laser greenhouse type of target to have an ablation pressure smaller (although insignificantly) than that of a direct-drive target, since the thermal mechanism for the absorption of laser radiation is at the basis of its operation, the necessary condition for which is $v_s/v_\kappa \leq 1$. At the same time, the condition for a thermal absorption mechanism is that there be no leakage of plasma from the absorber through the input apertures of the target within the time the laser pulse acts.

Despite the lower ablation pressure, the hydrodynamic compression efficiency of a laser greenhouse target exceeds the analogous quantity for a directly illuminated target because the ablation pressure is maintained after the end of the laser pulse, since the external inertial shell prevents the hydrodynamic expansion of the absorber. According to numerical calculations, the results of which are given in the next section, the hydrodynamic efficiency of a laser greenhouse target reaches values of 0.12 to 0.2.

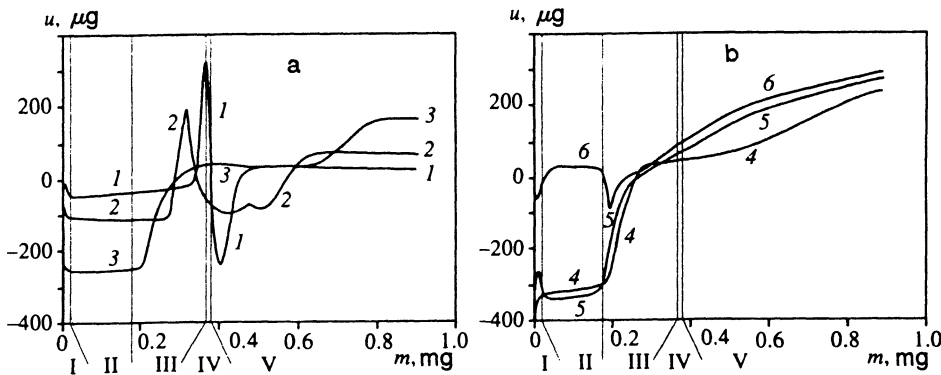


FIG. 2. Distribution of material velocities with respect to the target mass at successive times: For Fig. 2a, 1— $t=1$ ns, 2— $t=2$ ns, 3— $t=3$ ns; for Fig. 2b, 4— $t=4$ ns, 5— $t=5$ ns, 6— $t=5.4$ ns. The vertical lines along the mass coordinate axis show the separation of the target into structural regions: I—DT—ice II—copper layer, III—ablator (polyethylene), IV—absorber (porous polyethylene), V—external shell (polyethylene).

Note that for targets in which the symmetrization of the absorber heating is incomplete when the thermal waves exit the surface of the ablator, i.e., when $h \leq v_{\kappa} t_L$, according to (26) it is possible to achieve ablation pressures that considerably exceed the ablation pressure of a direct-drive target.

8. NUMERICAL CALCULATIONS FOR PROCESSES IN A LASER GREENHOUSE TARGET

At this time, researchers at the P. N. Lebedev Physical Institute and the Institute of Mathematical Simulation of the Russian Academy of Sciences are conducting an extensive investigation of the physical properties of laser greenhouse targets using one-dimensional and two-dimensional numerical calculations. In this paper we present the results of one-dimensional calculations, which we have used to optimize the target parameters. These data illustrate the physics described above for this type of target and confirm the conclusions of our theoretical analysis.

We would like to mention that preliminary two-dimensional calculations based on the "ATLANT" code²² showed efficient equalization of nonuniformities in the distribution of absorbed laser energy even for six laser beams.

One-dimensional numerical calculations were performed using the standard version of the "DIANA" code,²³ which describes the hydrodynamic motion of a two-temperature plasma with electron and ion thermal conductivity, bremsstrahlung and resonant absorption of laser radiation in the plasma, transport of intrinsic radiation in the three-temperature approximation, transport of α particles using one group in energy and two groups in angle, and other processes.

The cycle of calculations was performed for a wide range of laser radiation and target parameters. The energy of the laser radiation was varied from 0.5 to 1 MJ, the wavelength from 0.35 to 1.06 μm , and the pulse duration from 2 to 8 ns. We should mention first that the calculations demonstrated that the target had a high energy efficiency. Ignition of the target (a gain equal to 1) corresponded to a laser radiation energy of around 0.1 MJ; for laser energies of 1 MJ the gain coefficient was about 50.

As an example, consider the results of calculations for a target with parameters corresponding to ignition. The energy of the laser pulse in this calculation was 100 kJ, the wavelength was 1.06 μm , and the laser pulse, whose power increased linearly, had a duration of 3 ns.

The target had an inner ablator shell with an external radius of 1016 μm , consisting of an outer layer of plastic in its normal state ($\rho_0 = 1 \text{ g/cm}^3$) with a thickness of 15 μm and a thin inner layer of copper ($\rho_0 = 8.93 \text{ g/cm}^3$); the thickness of the DT ice layer ($\rho_0 = 0.2 \text{ g/cm}^3$) frozen onto the inner surface of the ablator was 8 μm ; the inner cavity of the working target was occupied by DT gas with a density of $\rho_0 = 10^{-4} \text{ g/cm}^3$. The outer inert shell had an external radius of 1533 μm , and consisted of an external layer of copper with thickness 2 μm and a layer of plastic in the normal state with a thickness of 22 μm . The absorber consisted of a layer of porous plastic with density $\rho_0 = 10^{-3} \text{ g/cm}^3$ and thickness 493 μm .

The calculations were performed in the two-temperature approximation, taking into account bulk losses via radiation. For this problem, the treatment of radiation was more suitable for this model than was for the three-temperature approximation.

In Fig. 2 we show the distribution of velocities for the target material versus the mass coordinate for the initial (Fig. 2a) and final (Fig. 2b) stages of target compression. The velocity profiles are shown for all the target layers except the outer copper shell. It is clear that in the initial stage, the target dynamics are characterized by counterpropagating expansion into the absorber region of both ablator material and material from the outer shell. The unevaporated layer of the internal target accelerates to the end of the laser pulse up to velocities of 250 km/s. The final compression velocity for the working target (Fig. 2b) reaches roughly 400 km/s.

In Fig. 3 we show the distribution of density with respect to target mass under the same conditions for the same target and times as in Fig. 2. These figures illustrate the dynamics of evaporation of target layers and the evolution of the density in the burned-through hot regions.

Figure 4 shows the temperature distribution for electrons in the absorber and the surrounding shell material at various instants of time. These data show the dynamics as the electron thermal-conduction wave develops in the radial direction. By the time the laser pulse ends (3 ns), the absorber temperature has reached a maximum of order 2.5 keV. After this, the average temperature of the burned-through layers falls, and the masses of these layers increase only slightly. In this case the fraction of evaporated ablator mass reaches 57%, the ablator pressure reaches 35 Mbar, and the hydrodynamic efficiency reaches $\eta = 10.5\%$. The energy loss via

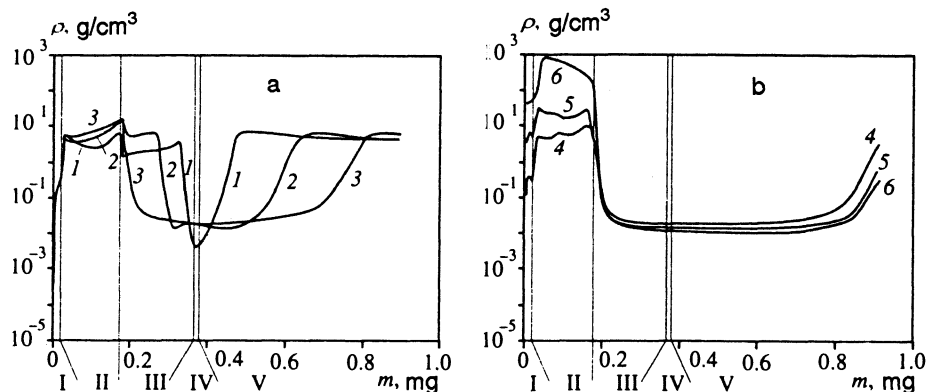


FIG. 3. Dependence of the density of target material on the mass coordinate at successive times: for Fig. 3a, 1— $t=1$ ns, 2— $t=2$ ns, 3— $t=3$ ns; for Fig. 3b, 1— $t=4$ ns, 2— $t=5$ ns, 3— $t=5.4$ ns.

radiation from the hot regions of the target at time 3 ns amounts to 1.24 kJ, and increases until the instant of collapse $t=t_c=5.40$ ns up to 2.73 kJ, i.e., it is less than 3% of the deposited energy.

The conditions for burning a DT plasma are illustrated in Fig. 5, where we show the profile of the ion temperature and density of the compressed material in the thermonuclear capsule at the instant of collapse $t=t_c$. When the average density in the thermonuclear plasma reaches a value $\rho_{DT}=56.0$ g/cm³ and a temperature $T_i = 5.45$ keV, the parameter $\rho R_{DT}=0.20$ g/cm³ at this instant. The gain coefficient for this target is 1.27.

9. CONCLUSIONS

The theoretical analysis given here and the results of numerical calculations show that the laser greenhouse target is capable of ensuring uniform distributions of the laser energy absorbed in the target and the pressure compressing the thermonuclear material. Targets of this type have excellent energy characteristics: ignition of the target corresponds to a laser radiation energy of 100 to 200 kJ, while an energy 1 MJ corresponds to a gain of 50. These characteristics exceed published data for targets of other types, either direct or indirect.

When a laser greenhouse target is used for which the absorber of laser radiation has subcritical density, bulk inverse bremsstrahlung absorption of laser radiation can occur in the thermal regime. This leads to conversion of up to 70 to 75% of the absorbed energy into thermal energy and the initiation of a supersonic electron thermal-conduction wave that equalizes heating nonuniformities in the absorber material; moreover, ablation pressures reach 20 to 40 Mbar and hydrodynamic efficiencies for accelerating the shell of the thermonuclear target reach 0.1 to 0.25 for moderate aspect ratios of the thermonuclear capsule, smaller than 50.

Investigation of the physics of the laser greenhouse target will involve an extensive program of experiments. The majority of the fundamental problems can be investigated using experiments with planar targets illuminated by one or two beams from a Nd laser (second and third harmonic) with relatively low energies (100 to 1000 J). Problems needing study are: deposition of energy in the target, and its absorption in a low-density or granular material; achievement of high concentrations of energy and plasma temperatures of several keV; electronic thermal conduction and equalization of plasma heating nonuniformities within the cavity at a temperature of 1 to 3 keV, including the possible effect of spontaneous magnetic fields; energy loss through the holes that admit the radiation; determining the real nonuniformities in the plasma heating within the cavity; the possibility of con-

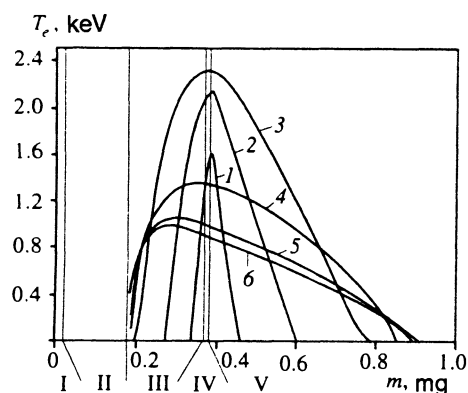


FIG. 4. A distribution of electron temperature with respect to target mass at successive times: 1— $t=1$ ns, 2— $t=2$ ns, 3— $t=3$ ns (when the pulse ends) and 4— $t=4$ ns, 5— $t=5$ ns, 6— $t=5.4$ ns (when the target collapses).

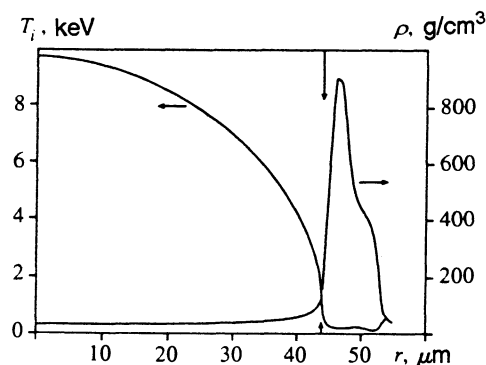


FIG. 5. Plot of ion temperature and matter density in the DT fuel and the copper layer versus target radius at time $t=t_c=5.4$ ns. The DT-Cu boundary is denoted by the vertical arrows.

trolling the radiation and plasma entropy; and the possibility of hydrodynamically compensating variations in the illumination due to the target structure.

Systems which can be used to test the basic principles of a spherical laser greenhouse target experimentally at laser energies of 10 to 20 kJ are: the Iskra-5 apparatus at the Arzamas-16 Federal Nuclear Center (Russia), the Phoebus laser at the Center for Research in Limeil-Valenton (France), and the Gekko-12 laser at the Osaka University Institute of Laser Engineering (Japan).

Finally, there remains the problem of developing the technology for making a laser greenhouse target. Here we must mention significant progress at the present time in the technology for fabricating layers of porous materials²⁴ with macrodensities down to 10^{-3} g/cm³.

Laser greenhouse targets of simplified design can be used to carry out interesting experimental studies of the physics of thermal equalization and hydrodynamic compensation of heating of a plasma by laser radiation laser beams. The first target of this kind should be a target without the external inertial shell, i.e., simply a capsule containing thermonuclear combustion material surrounded by an absorber made of porous material with subcritical macrodensity. The second type would be a target in which a gas of light elements, e.g., hydrogen or deuterium, with a subcritical density, serves as the absorber. In this target, the outer shell merely plays the functional role of the outer wall of the container that confines the gaseous absorber material. This shell can be made without input holes, but it should be thin so that it can evaporate within a time considerably shorter than the duration of the laser pulse. The outer shell should also be made of light-element material in order to ensure a low level of intrinsic radiation.

The preliminary two-dimensional numerical calculations we have performed for such targets have demonstrated a super-sonic thermal-conduction equalization of the temperature distribution of the plasma in the region where the radiation of the laser beams is absorbed.

In conclusion, we are deeply grateful to our co-workers G. A. Vergunova, N. N. Demchenko, I. G. Lebo, and Yu. A. Merkyul'ev at the Institute of Physics of the Russian Academy of Sciences for useful discussions of the results of this work.

- ¹ Yu. V. Afanas'ev, E. G. Gamaliĭ, O. N. Krokhin, V. B. Rozanov, *J. Appl. Math. Mech.* **39**, 451 (1975) [in Russian].
- ² Y. Kato, K. Mima, N. Miyanaga *et al.*, *Phys. Rev. Lett.* **53**, 1057 (1975).
- ³ S. Scupsky, R. W. Short, T. Kessler *et al.*, *J. Appl. Phys.* **68**, 3456 (1984).
- ⁴ S. Nakai, *Nucl. Fusion* **30**, 1779 (1990).
- ⁵ J. D. Lindl, R. L. McCrory, and E. M. Campbell, *Physics Today* **49**, 32 (1992).
- ⁶ J. Nuckols, *Physics Today* **9**, 25 (1982).
- ⁷ C. Yamanaka, in: *Proc. 10th IAEA Conf. on Plasma Phys. and Controlled Nuclear Fusion Research* (London, 1984), Vol. 3, p. 3 (1985).
- ⁸ M. M. Basko and J. Meyer-ter-Vehn, *Nucl. Fusion* **33**, 601 (1993).
- ⁹ N. G. Basov, S. Yu. Gus'kov, G. V. Danilova *et al.*, *Kvant. Elektron.* (Moscow) **12**, 1289 (1985) [*Sov. J. Quantum Electron.* **15**, 852 (1985)].
- ¹⁰ M. Andre, J. Coutant, and R. Dautray, in: *Proc. 14th Int. Conf. on Plasma Phys. and Controlled Nuclear Fusion Research* (Wurtzburg, 1992), Vol. 3, p. 23 (1993).
- ¹¹ S. Yu. Gus'kov and V. B. Rozanov, in: Abstracts, *All-Russia Conf. on Plasma Physics and Controlled Thermonuclear Fusion* (Zvenigorod, 1994) [in Russian].
- ¹² S. Yu. Gus'kov, V. B. Rozanov, and N. V. Zmitreko, in: Abstracts, *ECLIM '94 Conf.* (Oxford, Sept. 1994), PA-17.
- ¹³ W. L. Kruer, in: *Laser Plasma LLNL Annual Report No. UCRL-50021-80*, Sec. 3, p. 25 (1980).
- ¹⁴ Yu. V. Afanas'ev and S. Yu. Gus'kov, in: *Nuclear Fusion by Inertial Confinement*, G. Velarde *et al.*, p. 99 (CRC Oress, 1993).
- ¹⁵ N. G. Basov and O. N. Krokhin, *Zh. Éksp. Teor. Fiz.* **46**, 171 (1964) [*Sov. Phys. JETP* **19**, 123 (1964)].
- ¹⁶ Yu. V. Afanas'ev, E. G. Gamaliĭ, S. Yu. Gus'kov *et al.*, *Laser and Particle Beams* **6**, 1 (1988).
- ¹⁷ Yu. V. Afanas'ev, E. G. Gamaliĭ, and V. B. Rozanov, *Proc. P. N. Lebedev Inst. of Phys., Russian Acad. Sci. (FIAN)* **134**, 10 (Moscow, 1982) [in Russian].
- ¹⁸ Ya. B. Zel'dovich and Yu. P. Raizer, *Physics of Shock Waves and High-Temperature Hydrodynamic Phenomena*, Academic, New York (1966-67).
- ¹⁹ N. G. Basov, G. A. Vergunova, and V. B. Rozanov, *Zh. Éksp. Teor. Fiz.* **84**, 564 (1983) [*Sov. Phys. JETP* **57**, 325 (1983)].
- ²⁰ L. D. Landau, *Zh. Éksp. Teor. Fiz.* **7**, 203 (1937)
- ²¹ P. P. Volosevich, S. P. Kudryumov, E. I. Levanov, *Appl. Math. Theor. Phys.* **5**, 41 (1972) [in Russian].
- ²² E. G. Gamaliĭ, N. N. Dauchenko, I. G. Ledo *et al.*, *Kvant. Elektron.* (Moscow) **15**, 1622 (1988) [*Sov. J. Quantum Electron.* **18**, 1012 (1988)].
- ²³ A. A. Samarskiĭ, S. N. Gaifulin, N. V. Zakarov *et al.*, in the collection: *Problems in Atomic Science and Technology: Problems in Nuclear Physics and Engineering* **2**, p. 38, E. P. Vashkova, ed. (Energoizdat, Moscow, 1983) [in Russian].
- ²⁴ N. G. Borisenko and Yu. A. Merkul'ev, *Proc. P. N. Lebedev Inst. of Phys., Russian Acad. Sci. (FIAN)* **220**, 28 (Moscow, 1992) [in Russian].

Translated by Frank J. Crowne